Speed Estimation in Wireless Systems Using Wavelets

Ravi Narasimhan and Donald C. Cox, *Fellow, IEEE*

***Abstract*— A new technique is described for estimating the speed of a mobile station in a wireless system. The mobile speed maps the characteristic spatial scale of the received signal into a characteristic temporal scale. The continuous wavelet transform tracks changes in the temporal scale to estimate the mobile speed as a function of time. This technique requires neither knowledge of the average received power of the nonstationary signal nor adaptation of a temporal observation window, in contrast to other speed estimators given in the literature. Simulations show the tracking of a variable speed profile.**

***Index Terms*—Speed estimation, velocity estimation, wavelets, wireless communication.**

I. Introduction

A SIGNIFICANT characteristic of wireless systems is the signal variation caused by the movement of the mobile stations. Estimating the speed of a mobile station is desirable for several reasons. One application of speed estimation is to determine the duration of a temporal window over which the received signal is averaged to mitigate signal variation. Mobile speed can also be used to determine whether a mobile station that requests access to the wireless system should be assigned to a microcell (for low mobile speeds) or to an umbrella macrocell (for high mobile speeds). System control algorithms, such as handoff algorithms, can also benefit from knowledge of mobile speed.

In many environments, a direct path is not present between the base station and the mobile station. The received signal consists of a sum of waves that have been reflected by objects such as mountains, trees, and buildings. The sum of many waves at the receiver gives rise to small-scale spatial variation of the received signal (on the order of a wavelength). In situations where there is no dominant path between the base station and the mobile station, the small-scale spatial variation is called Rayleigh fading [1]. The received signal is nonstationary for distances on the order of building sizes, since the mean of the small-scale variation changes considerably. This large-scale variation of the mean is known as shadowing. The mean of the shadowing also decreases as the distance between the base station and the mobile station increases.

Estimates of the mobile speed can be obtained by using the statistics of the received signal. For example, level crossing rates [2] or the autocovariance [3] of the received envelope have been used to estimate speed. Speed estimates have also been obtained by estimating the maximum Doppler frequency using eigenspace methods [4], spectrum estimation methods [5], and the squared deviations of the logarithmically compressed envelope [6]. Another method of velocity estimation requires knowledge of the average signal strength for all locations within a region of interest and uses a technique similar to the multidimensional scaling method of statistical data analysis [7]. All of the above techniques require estimates of the signal power, and some methods also require the signal autocorrelation. A difficulty in obtaining such estimates is the nonstationary nature of the received signal. An appropriate window which depends on the unknown mobile speed must be chosen to estimate the required quantities. Furthermore, the above-mentioned literature has considered only the problem of a constant, unknown mobile speed. For variable speeds, the duration of the observation window must be constantly adapted, and the rate of adaptation will be critical to the performance of the speed estimator. In particular, errors in the speed estimates could propagate due to suboptimal observation windows.

A new method of speed estimation using wavelets is described in this paper. The wavelet transform at different scales corresponds to a variety of window lengths and, hence, eliminates the necessity of adapting the duration of a single temporal observation window. The method presented here utilizes the fact that the small-scale spatial variation of the received envelope is dominated by the positions of the mobile and base stations. This spatial variation has a characteristic scale that is on the order of a carrier wavelength. The temporal variation of the received envelope is then a consequence of mapping the spatial variation through the mobile speed. By tracking the characteristic temporal scale of the variations, an estimate of the speed is obtained as a function of time.

The paper is organized as follows. In Section II, a wireless propagation model is presented. Section III presents a method for speed estimation using the continuous wavelet transform (CWT). Section IV addresses the selection of parameters used in the speed estimate, compares the performance with other estimators for constant mobile speed, and gives results of simulations using variable mobile speeds. Conclusions are given in Section V.

Paper approved by S. Ariyavisitakul, the Editor for Wireless Techniques and Fading of the IEEE Communications Society. Manuscript received August 19, 1998; revised January 4, 1999 and February 23, 1999. This work was supported by Nortel, the Okawa Foundation, and a National Science Foundation Graduate Research Fellowship. This paper was presented in part at the IEEE International Conference on Communications (ICC), Vancouver, British Columbia, Canada, June 1999.

The authors are with the Department of Electrical Engineering, Stanford University, Stanford, CA 94305-9515 USA (e-mail: nkravi@wireless.stanford.edu; dcox@nova.stanford.edu).

Publisher Item Identifier S 0090-6778(99)07462-0.

II. Wireless Propagation Model

The propagation model discussed here takes into account three effects which are present in many wireless environments: correlated Rayleigh fading, correlated lognormal shadowing, and a distance-dependent trend. The received bandpass signal at a mobile consists of a sum of contributions from several paths. Let $T_c(\mathbf{x})$ and $T_s(\mathbf{x})$ denote the inphase and quadrature components of the received signal at position $\mathbf{x}$. By the central limit theorem, $T_c(\mathbf{x})$ and $T_s(\mathbf{x})$ are independently, identically distributed (i.i.d.) wide-sense stationary, zero-mean Gaussian random processes in a small neighborhood of $\mathbf{x}$. The size of the neighborhood of $\mathbf{x}$ is much smaller than the size of buildings. The power density incident upon the receiver is assumed to be uniformly distributed in angle in a plane. Let $p(\mathbf{x}, \mathbf{x_B})$ denote the received power at the mobile station averaged over a small neighborhood of $\mathbf{x}$ due to a base station located at $\mathbf{x_B}$. Let λ represent the carrier wavelength. Under the above conditions and for an omnidirectional antenna, the auto and cross correlations of $T_c(\mathbf{x})$ and $T_s(\mathbf{x})$, in the direction $\hat{\mathbf{u}}$, and in a small neighborhood of $\mathbf{x}$ are given by [1]

$$\begin{aligned} R_{T_c}(y, p(\mathbf{x}, \mathbf{x_B})) &\equiv E\{T_c(\mathbf{x} + y\hat{\mathbf{u}})\, T_c(\mathbf{x})\} \\ &= R_{T_s}(y, p(\mathbf{x}, \mathbf{x_B})) \\ &= p(\mathbf{x}, \mathbf{x_B})\, J_0(2\pi y/\lambda) \qquad (1) \\ R_{T_c T_s}(y, p(\mathbf{x}, \mathbf{x_B})) &\equiv E\{T_c(\mathbf{x} + y\hat{\mathbf{u}})\, T_s(\mathbf{x})\} \\ &= 0 \qquad (2) \end{aligned}$$

where $J_0(\cdot)$ denotes the zeroth-order Bessel function of the first kind. The auto and cross correlations explicitly indicate the fact that $T_c(\mathbf{x})$ and $T_s(\mathbf{x})$ are wide-sense stationary only in a small neighborhood of $\mathbf{x}$. Let $\langle \mathbf{a}, \mathbf{b} \rangle$ denote the inner product between vectors $\mathbf{a}$ and $\mathbf{b}$. A model for $T_c(\mathbf{x})$ and $T_s(\mathbf{x})$ (for travel in the direction $\hat{\mathbf{u}}$) can be shown to be

$$\hat{T}_c(\mathbf{x}) = \left[\frac{2p(\mathbf{x}, \mathbf{x_B})}{K}\right]^{1/2} \cdot \sum_{j=0}^{K-1} \cos\left\{\frac{2\pi\langle \mathbf{x}, \hat{\mathbf{u}}\rangle}{\lambda}\left[\cos\left(\frac{\pi(j+1/2)}{K}\right)\right] + \theta_j(\mathbf{x}, \mathbf{x_B})\right\} \qquad (3)$$

$$\hat{T}_s(\mathbf{x}) = \left[\frac{2p(\mathbf{x}, \mathbf{x_B})}{K}\right]^{1/2} \cdot \sum_{j=0}^{K-1} \cos\left\{\frac{2\pi\langle \mathbf{x}, \hat{\mathbf{u}}\rangle}{\lambda}\left[\cos\left(\frac{\pi(j+1/2)}{K}\right)\right] + \phi_j(\mathbf{x}, \mathbf{x_B})\right\} \qquad (4)$$

where K is the number of terms in the model, and $\theta_j(\mathbf{x}, \mathbf{x_B})$ and $\phi_j(\mathbf{x}, \mathbf{x_B})$ are i.i.d. uniformly on $[0, 2\pi)$.

The average received power $p(\mathbf{x}, \mathbf{x_B})$ contains the distance-dependent trend and lognormal shadowing [8]. Let α represent the exponent of the distance-dependent trend. Furthermore, let $10^{L(\mathbf{x}, \mathbf{x_B})/10}$ denote the lognormal shadowing between the mobile position $\mathbf{x}$ and the base station position $\mathbf{x_B}$. The received power averaged over a neighborhood of $\mathbf{x}$ due to the base station located at $\mathbf{x_B}$ can then be expressed as

$$p(\mathbf{x}, \mathbf{x_B}) = P_0 \|\mathbf{x} - \mathbf{x_B}\|^{-\alpha} 10^{L(\mathbf{x}, \mathbf{x_B})/10} \qquad (5)$$

where P_0 accounts for antenna parameters, transmitted power, and other relevant system parameters. The process $L(\mathbf{x}, \mathbf{x_B})$ is modeled as a zero-mean Gaussian random process that is wide-sense stationary in the variable $\mathbf{x}$. Let $R_L(y, \mathbf{x_B})$ denote the autocorrelation of $L(\mathbf{x}, \mathbf{x_B})$ in the variable $\mathbf{x}$ along the direction $\hat{\mathbf{u}}$. An empirical model for $R_L(y, \mathbf{x_B})$ is [9]

$$R_L(y, \mathbf{x_B}) = \sigma_L^2(\mathbf{x_B}) \exp\left(-\frac{|y|}{d_0(\mathbf{x_B})}\right) \qquad (6)$$

where $\sigma_L^2(\mathbf{x_B})$ and $d_0(\mathbf{x_B})$ are the variance and correlation length of $L(\mathbf{x}, \mathbf{x_B})$. The power spectrum $S_L(\nu, \mathbf{x_B})$ of $L(\mathbf{x}, \mathbf{x_B})$ is given by

$$S_L(\nu, \mathbf{x_B}) = \frac{2d_0(\mathbf{x_B})\sigma_L^2(\mathbf{x_B})}{1 + [2\pi\nu d_0(\mathbf{x_B})]^2} \qquad (7)$$

where ν denotes spatial frequency. Let $\nu_{\max}$ denote the maximum spatial frequency of $S_L(\nu, \mathbf{x_B})$ that is taken into account, and let D be the magnitude of the total displacement of the mobile within a time period of interest. A model for the process $L(\mathbf{x}, \mathbf{x_B})$ can be shown to be

$$\hat{L}(\mathbf{x}, \mathbf{x_B}) = \sum_{j=-J}^{J-1} \left[\frac{2}{CD} S_L\left(\frac{(j+1/2)}{D}, \mathbf{x_B}\right)\right]^{1/2} \cdot \cos\left[\frac{2\pi\langle \mathbf{x}, \hat{\mathbf{u}}\rangle}{D}(j+1/2) + \beta_j(\mathbf{x}, \mathbf{x_B})\right] \qquad (8)$$

where

$$C = \frac{1}{D\sigma_L^2(\mathbf{x_B})} \sum_{j=-J}^{J-1} S_L\left(\frac{(j+1/2)}{D}, \mathbf{x_B}\right) \qquad (9)$$

$$\nu_{\max} = J/D$$

and $\beta_j(\mathbf{x}, \mathbf{x_B})$ are i.i.d. uniformly on $[0, 2\pi)$. The received envelope is Rayleigh distributed. The received signal envelope $r(\mathbf{x})$ and its logarithm $s(\mathbf{x})$ are then given by

$$r(\mathbf{x}) = \sqrt{\hat{T}_c^2(\mathbf{x}) + \hat{T}_s^2(\mathbf{x})} \qquad (10)$$

$$s(\mathbf{x}) = 20\log_{10}[r(\mathbf{x})]. \qquad (11)$$

The model presented here is used in the speed estimation method described in Section III.

III. Speed Estimation Using CWT

The speed estimation technique presented here utilizes the characteristic spatial scale due to correlated Rayleigh fading of the received signal. In this analysis, the signal of interest is the logarithm of the envelope. Let the curve Γ traversed by the mobile station be parametrized by the scalar position variable x, and let $g(x)$ represent the received signal (i.e., the logarithm of the envelope) as a function of x. Fig. 1 plots a typical signal trace as a function of distance (measured in wavelengths). This plot shows that the local minima of the signal occur with a separation of a fraction of a wavelength. Suppose that the mobile travels along Γ with a speed $v(t)$ at time t. The received signal $f(t)$ as a function of t is then

$$f(t) = g\left(\int_0^t v(t')\, dt'\right), \qquad t \geq 0 \qquad (12)$$

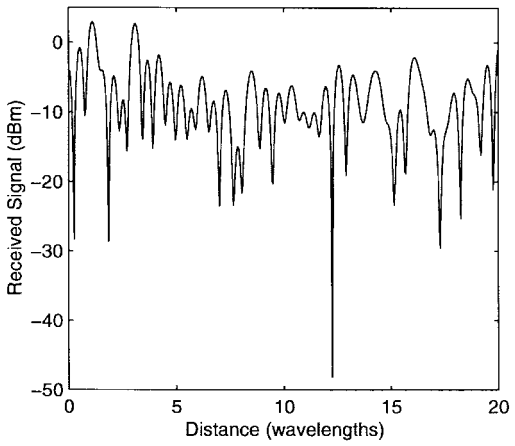

Fig. 1. Typical signal trace as a function of distance.

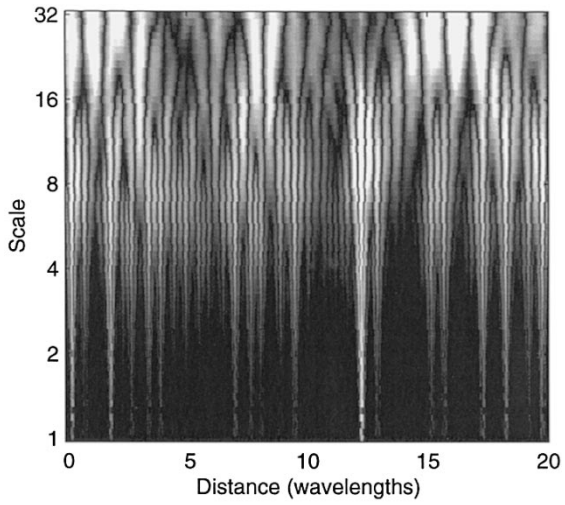

Fig. 2. Absolute value of CWT of signal given in Fig. 1. White represents large magnitude and black represents small magnitude.

where we have taken the time origin to correspond to $x = 0$. This model accounts for Rayleigh fading in the absence of additive noise. Let the mean separation in distance between the local minima of $g(x)$ be $k\lambda$ where $0 < k < 1$. If the mean separation in a neighborhood of time t between the local minima of $f(t)$ is $\Delta T(t)$, an estimate $\hat{v}(t)$ for the speed can be obtained as

$$\hat{v}(t) = \frac{k\lambda}{\Delta T(t)}. \tag{13}$$

A method to estimate $\Delta T(t)$ using the CWT is described in the following.

The CWT of a function $h(t) \in L_2(\mathcal{R})$ is given by

$$\mathrm{CWT}_h(a,b) \equiv \frac{1}{\sqrt{a}} \int_{-\infty}^{\infty} \psi\left(\frac{t-b}{a}\right) h(t)\, dt \tag{14}$$

where $a \in \mathcal{R}^+$ denotes "scale" and $b \in \mathcal{R}$ denotes "shift." The "mother wavelet" $\psi(t) \in L_2(\mathcal{R})$ is taken to be real and satisfies the admissibility condition

$$C_\psi = \int_0^{\infty} \frac{|\Psi(\omega)|^2}{|\omega|}\, d\omega = \int_{-\infty}^{0} \frac{|\Psi(\omega)|^2}{|\omega|}\, d\omega < \infty \tag{15}$$

where $\Psi(\omega)$ is the Fourier transform of $\psi(t)$. Fig. 2 plots the absolute value of a CWT of the signal given in Fig. 1.

The CWT has the important property of characterizing singularities of the signal $h(t)$ [10]–[12]. Let all derivatives of $h(t)$ up to order n exist and be of bounded variation. If the nth derivative of $h(t)$ is discontinuous at $t = t_0$, then for a constant c_n, $\mathrm{CWT}_h(a, t_0) \simeq c_n a^{n+1/2}$ as $a \to 0$. As shown in Fig. 1, many of the local minima of $g(x)$ correspond to points of discontinuity in the first derivative. Thus, the CWT behaves as $a^{3/2}$ for small a near the local minima of $g(x)$ with discontinuous derivative.

The CWT is applied to the received signal $f(t)$ in order to detect the points of discontinuity in the first derivative of $f(t)$. In order to obtain speed estimates within an acceptable delay for real-time implementation, the CWT of $f(t)$ is taken over a suitable temporal window of observation. The CWT is taken at a discrete set of scales $a = 2^{j+m/M}$, $j = j_{\min}, j_{\min}+1, \cdots, j_{\max}$, $m = 0, \cdots, M-1$ where $j_{\min}$, $j_{\max}$, and M are integers. In order to compare the CWT with a significance threshold which is independent of mobile speed, the CWT is normalized as follows. Let $f_0(t)$ be the received signal for a constant mobile speed v_0, and $f_1(t) = f_0(t/A)$ be the received signal for a constant mobile speed $v_1 = v_0/A$. Definition (14) relates the CWT's of $f_0(t)$ and $f_1(t)$

$$\mathrm{CWT}_{f_1}(a,b) = \sqrt{A}\, \mathrm{CWT}_{f_0}(a/A, b/A). \tag{16}$$

Thus, the CWT of $f(t)$ at each scale a is normalized by $1/\sqrt{a}$ before further processing.

One method to detect the points of discontinuity in the first derivative of $f(t)$ is to identify the wavelet transform modulus maxima [10]. The number of wavelet transform modulus maxima at fine scales, which are associated with a singularity of $f(t)$, depends upon the number of local extrema of the analyzing wavelet $\psi(t)$. The number of local extrema of the wavelet is at least one plus the number of vanishing moments of the wavelet. Furthermore, the analyzing wavelet must have at least two vanishing moments in order to characterize points of discontinuous derivative of $f(t)$. In order to reduce the number of extraneous wavelet transform modulus maxima which are associated with a singularity of $f(t)$, the following method is adopted. For wavelets $\psi(t)$ which satisfy $\sup_t \psi(t) \geq -\inf_t \psi(t)$, the *negative local minima* at each scale of the normalized CWT are identified; otherwise, the *positive local maxima* at each scale are identified. The values which are identified by the method described above will be referred to as the *signed local extrema* of the normalized CWT. The signed local extrema with absolute value less than a significance threshold τ are discarded. The scale which has the highest number of significant signed local extrema is identified as the scale of interest and is denoted by a_τ.

Since most of the local minima of $f(t)$ correspond to points of discontinuity in the first derivative, the locations in time of the signed local extrema of the normalized CWT correspond to most of the locations of the local minima of the signal $f(t)$. To compensate for the small fraction of local minima of $f(t)$ with continuous derivative, the significance threshold

τ is determined empirically such that the number of local minima of $f(t)$, which are detected by the CWT, is equal to the total number of local minima of $f(t)$. We now consider $(N+1)$ significant signed local extrema. For a fixed N, these signed local extrema correspond to a time interval $t \in [t_0, t_1]$, which depends on the mobile speed. Let ΔT_n denote the time between the $(n-1)$th and nth signed local extrema. The estimate (13) for $v(t)$ at time $(t_0+t_1)/2$ becomes

$$\hat{v}\left(\frac{t_0+t_1}{2}\right) = \frac{k\lambda}{\frac{1}{N}\sum_{n=1}^{N}\Delta T_n}. \tag{17}$$

The next speed estimate sample $\hat{v}((t_0'+t_1')/2)$ is obtained by averaging over a time interval $[t_0', t_1']$ which contains a new signed local extremum and the N most recent signed local extrema from the previous time interval. The speed estimates obtained in this manner are smoothed by a moving average. The following section describes the selection of parameters used in the above speed estimate together with simulations that apply the estimation technique.

IV. Parameter Selection and Simulation Results

This section addresses the determination of the mean distance between local minima of the signal $(k\lambda)$, the selection of the significance threshold (τ), and number (N) of interarrival times of the signed local extrema to be used in the speed estimate. The choice of the maximum scale $(a_{\max})$, the duration (T_{obs}) of the observation window over which the CWT is taken, and associated boundary effects are also described. The observation window is required to obtain speed estimates within an acceptable delay for real-time implementation. Finally, an application of the speed estimation technique is presented for constant speed and for a variable speed profile as a function of time.

A. Mean Distance Between Local Minima of the Signal

The mean distance between the adjacent local minima of $g(x)$ is determined by the mean distance between adjacent positive-slope zero crossings of the derivative $g'(x)$. As given in Section III, the mean distance between adjacent positive-slope zero crossings of $g'(x)$ is $k\lambda$. The constant k is determined by the reciprocal of the zero crossing rate (ZCR) of $g'(x)$. Details of the calculation are given in the Appendix. The resulting value for k is about 0.662.

B. Selection of Significance Threshold

The threshold τ is selected such that the largest number of significant signed local extrema that are detected at scale a_τ is equal to the number of positive-slope zero crossings of the derivative $g'(x)$. Fig. 3 plots the ratio of the number of significant signed local extrema detected to the number of positive-slope zero crossings of $g'(x)$ as a function of the threshold τ. The results shown here correspond to averages over ten independent realizations of the Rayleigh fading and lognormal shadowing processes, each realization using approximately 1000 positive-slope zero crossings of $g'(x)$. Each of the four curves corresponds to a different analyzing wavelet

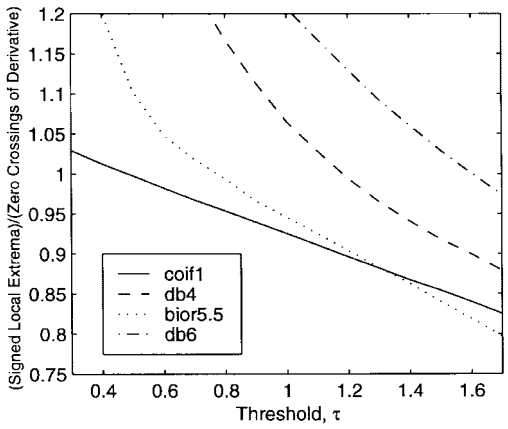

Fig. 3. Ratio of number of significant signed local extrema detected to the number of positive-slope zero crossings of signal derivative as a function of threshold.

$\psi(t)$. The wavelets chosen here are Daubechies' filters of order four (db4) and six (db6), a "coiflet" of order two (coif1), and a symmetric compactly supported biorthogonal spline wavelet (bior5.5) [11]. The optimum threshold for each wavelet is the value of τ for which the ordinate is 1.0 in Fig. 3. Table I summarizes some properties of the four analyzing wavelets and the corresponding optimum thresholds τ. In addition to the wavelets mentioned above, one of the wavelets described in [13] was also used. This wavelet has two vanishing moments and is constructed using maximally flat, discrete-time low-pass and high-pass filters with nine taps. The performance of this wavelet is similar to that of the coiflet (coif1).

The possibility of using the received envelope directly (instead of the logarithm of the envelope) was also investigated. One observation is that the local minima present in the envelope are not as prominent as those in the logarithm of the envelope. Furthermore, as the average received power $p(\mathbf{x}, \mathbf{x_B})$ decreases, the magnitude of the CWT of the envelope also decreases, while the magnitude of the CWT of the logarithm of the envelope does not depend on the absolute received power. Since the optimum threshold τ would depend on the absolute received power if the CWT were applied directly to the received envelope, the logarithm of the envelope is chosen for signal analysis.

C. Effect of Number of Interarrival Times on Speed Estimate

Fig. 4 plots the normalized bias of the speed estimate $E[\hat{v}/v] - 1$ as a function of the number of interarrival times (N) of adjacent signed local extrema for the four analyzing wavelets given in Table I. While the bias is negligible for large N, the value of N must be sufficiently small in order to track changes in mobile speed. Fig. 5 plots the normalized mean square error (MSE) of the speed estimate $E[(1-\hat{v}/v)^2]$ as a function of number of interarrival times. For a given number of interarrival times, the coiflet (coif1) performs better than the other wavelets. As mentioned in Section III, the coiflet performs well, since it has exactly two vanishing moments and, hence, minimizes the number of extraneous signed local extrema.

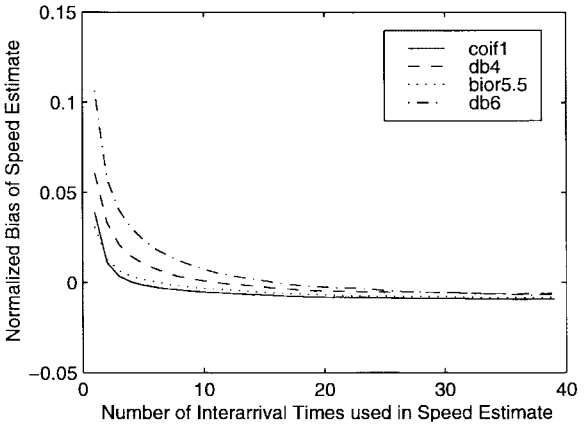

Fig. 4. Normalized bias versus number of interarrival times used in speed estimate.

TABLE I
PROPERTIES OF ANALYZING WAVELETS AND VALUES OF THRESHOLD

Wavelet	Vanishing Moments	Length of Support	τ
coif1	2	5	0.48
db4	4	7	1.18
bior5.5	6	9	0.78
db6	6	11	1.60

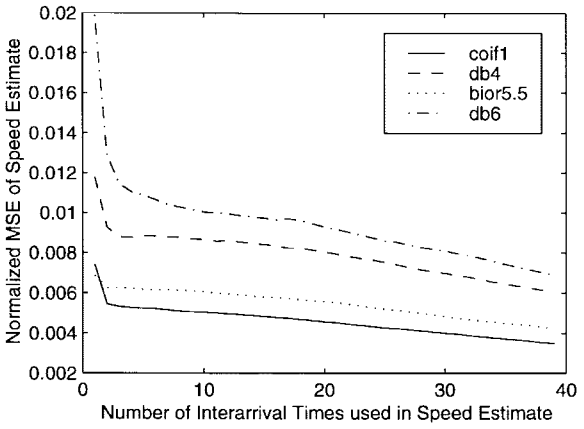

Fig. 5. Normalized MSE versus number of interarrival times used in speed estimate.

D. Choice of Maximum Scale, Duration of Observation Window, and Boundary Effects

The CWT is applied to blocks of the signal collected over time periods of duration $T_{\rm obs}$ in order to limit the delay in obtaining speed estimates for real-time implementation. The determination of $T_{\rm obs}$ is described in the following. Let the lowest speed of interest be denoted by $v_{\min}$, i.e., speeds less than $v_{\min}$ will be approximated by zero. If L_ψ denotes the duration of support of the analyzing wavelet $\psi(t)$, the maximum scale for the CWT is

$$a_{\max} = \frac{k\lambda}{L_\psi v_{\min}} \tag{18}$$

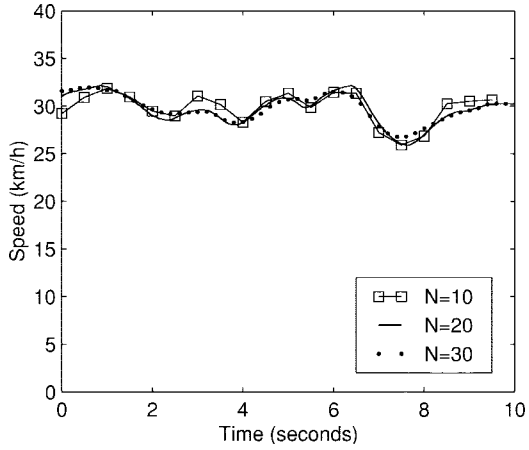

Fig. 6. Speed estimates using various numbers of interarrival times N for a constant mobile speed of 30 km/h.

where k is determined in Section IV-A. The duration of the observation window is then the duration of the coarsest wavelet, i.e., $T_{\rm obs} = L_\psi a_{\max}$. The finite observation window results in boundary effects in the detection of the signed local extrema. In order to remove these effects, the observation windows are enlarged by $T_{\rm obs}/2$ for each boundary (left and right endpoints). The enlarged windows slide by an amount $T_{\rm obs}$ as time progresses. For the initial left boundary and the final right boundary, the signal $f(t)$ is reflected about the boundaries such that $f(t)$ and the first derivative $f'(t)$ are continuous at the boundaries. This technique of overlapping windows results in a factor of two increase in computation for the CWT and a $T_{\rm obs}/2$ increase in delay of the speed estimate.

E. Application of Speed Estimation Technique

In this subsection, the speed estimation method is applied to specific functions of mobile speed versus time. Fig. 6 gives the estimated speed using various numbers of interarrival times N for a constant mobile speed of 30 km/h. The relevant parameters for this example, which uses the coif1 wavelet, are $v_{\min} = 0.72$ km/h, $\tau = 0.48$, and $M = 6$. The carrier wavelength is $\lambda = 1/3$ m, the correlation length of the lognormal shadowing is $d_0(\mathbf{x_B}) = 50$ m, and the exponent of distance dependence is $\alpha = 4$. The speed estimates were smoothed using a moving average of duration $T_{\rm obs}$.

In contrast to the level crossing and covariance methods given in [2], speed estimation using wavelets as described here does not require the design of temporal windows which must adapt sufficiently quickly to track the variation of mobile speed while being robust to the variability in the statistics used for speed estimation. Furthermore, since level crossing and covariance methods require estimates of the average received power, these speed estimators experience abrupt changes when the mobile makes a turn at a street corner. Since the method based on wavelets presented here does not require estimates of the average received power, there would be no sudden change in estimated speed at a street corner.

In order to demonstrate the tracking of changes in mobile speed, the speed estimator based on wavelets is applied to the

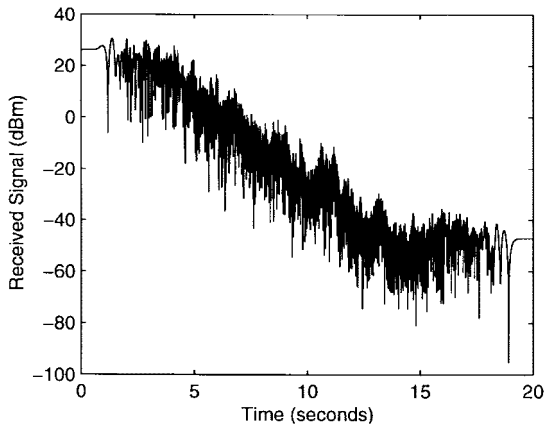

Fig. 7. Received signal for speed profile given in (19).

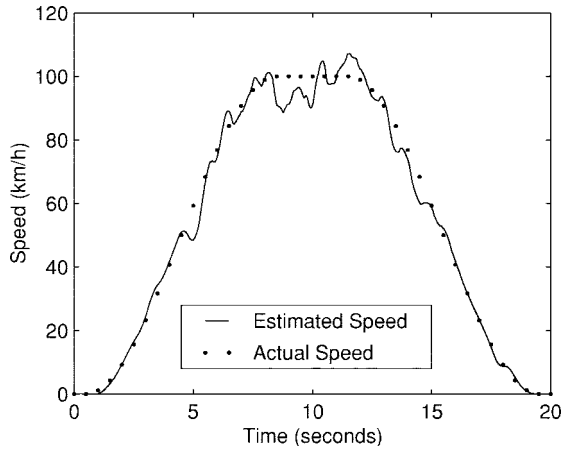

Fig. 8. Estimated speed and actual speed versus time.

following speed profile $v(t)$ (in km/h):

$$v(t) = \begin{cases} 0, & 0 \le t < 0.5 \\ 100\gamma\left(\dfrac{t-0.5}{8}\right), & 0.5 \le t < 8.5 \\ 100, & 8.5 \le t < 11.5 \\ 100\gamma\left(\dfrac{19.5-t}{8}\right), & 11.5 \le t < 19.5 \\ 0, & 19.5 \le t \le 20 \end{cases} \tag{19}$$

where

$$\gamma(t) = \begin{cases} 0, & t < 0 \\ 3t^2 - 2t^3, & 0 \le t < 1 \\ 1, & 1 \le t. \end{cases} \tag{20}$$

Fig. 7 plots the logarithm of the received envelope as a function of time for the speed profile $v(t)$ given above. Fig. 8 plots the actual speed $v(t)$ and the estimate $\hat{v}(t)$. For this example, the parameters are the same as those used in Fig. 6 except $v_{\min} = 1.8$ km/h and $N = 20$ (i.e., a maximum of $N + 1 = 21$ signed local extrema are used in the speed estimate; the actual number of signed local extrema used in a neighborhood of time t depends on the speed $v(t)$ and the duration of the observation window T_{obs}).

A fundamental quantity in evaluating the performance of the estimator is the normalized MSE as a function of the number of interarrival times N (Fig. 5). While the absolute MSE of the speed estimate depends on the mobile speed, the normalized MSE is fixed for a given N. This behavior is important for channel assignment and handoff algorithms whose performances depend on the spatial variation of the signal. It would be useful to compare this estimator with other techniques; however, other papers have not given algorithms for estimating variable mobile speeds. As shown in Fig. 8, the speed estimator presented here is able to track the changes in the mobile speed well.

V. Conclusion

The paper presents a new technique for estimating mobile speed in a Rayleigh fading environment. A wireless propagation model is proposed which accounts for correlated Rayleigh fading, correlated lognormal shadowing, and a distance-dependent trend. The characteristic spatial scale of the signal is mapped into a characteristic temporal scale through the mobile speed. With an empirically determined significance threshold, the significant signed local extrema of the CWT are used to detect the local minima in the logarithm of the received envelope. The interarrival times of adjacent signed local extrema are used to obtain an estimate of the mobile speed. Computer simulations indicate that the estimate is able to track a realistic, variable speed profile.

Appendix

The positive-slope ZCR of $g'(x)$ is determined using the propagation model of Section II. In a neighborhood of position $\mathbf{x}$ and with respect to a base station located at $\mathbf{x_B}$, we let (following the notations of [14]) $b_0 \equiv p(\mathbf{x}, \mathbf{x_B})$, $b_2 = \frac{b_0}{2}(2\pi/\lambda)^2$, and $b_4 = \frac{3b_0}{8}(2\pi/\lambda)^4$. Let x denote a small distance from position $\mathbf{x}$, and let $T_c(x)$, $T_s(x)$, $r(x)$, and $\Theta(x)$ denote the inphase component, quadrature component, envelope and phase of the received signal. Since $g(x)$ is the logarithm of the envelope, the ZCR of $g'(x)$ is equal to that of $r'(x)$. The positive-slope ZCR of $r'(x)$ is given by

$$\text{ZCR}_{r'(x)} = \int_0^\infty r''\rho(r' = 0, r'')\, dr'' \tag{21}$$

where $\rho(r', r'')$ is the joint probability density function (pdf) of $r'(x)$ and $r''(x)$. The ZCR is determined by the change of variables $(T_c, T_s, T_c', T_s', T_c'', T_s'') \to (r, \Theta, r', \Theta', r'', \Theta'')$. The Jacobian of this transformation is r^3. The vector $\mathbf{z} \equiv [T_c, T_s, T_c', T_s', T_c'', T_s'']^T$ is a zero-mean Gaussian random vector with covariance

$$\Sigma = \begin{bmatrix} b_0 & 0 & 0 & 0 & -b_2 & 0 \\ 0 & b_0 & 0 & 0 & 0 & -b_2 \\ 0 & 0 & b_2 & 0 & 0 & 0 \\ 0 & 0 & 0 & b_2 & 0 & 0 \\ -b_2 & 0 & 0 & 0 & b_4 & 0 \\ 0 & -b_2 & 0 & 0 & 0 & b_4 \end{bmatrix}. \tag{22}$$

The pdf of $\mathbf{z}$ is then

$$\rho(\mathbf{z}) = \frac{1}{(2\pi)^3|\Sigma|^{1/2}} \exp\left[-\frac{1}{2}\mathbf{z}^T\Sigma^{-1}\mathbf{z}\right]. \tag{23}$$

$$\rho(r,\Theta,r',\Theta',r'',\Theta'') = \frac{r^3}{(2\pi)^3 b_2\left(b_0b_4-b_2^2\right)}\exp\Bigg\{-\frac{1}{2b_2\left(b_0b_4-b_2^2\right)}\left[b_2b_4r^2 - b_2^2(r')^2 + b_0b_4(r')^2 + 2b_2^2rr'' + b_0b_2(r'')^2 - 3b_2^2r^2(\Theta')^2 + b_0b_4r^2(\Theta')^2 + 4b_0b_2(r')^2(\Theta')^2 - 2b_0b_2rr''(\Theta')^2 + b_0b_2r^2(\Theta')^4 + 4b_0b_2rr'\Theta'\Theta'' + b_0b_2r^2(\Theta'')^2\right]\Bigg\}. \tag{24}$$

$$\begin{aligned}\rho(r,r'=0,r'') &= \int_{\Theta=0}^{2\pi}\int_{\Theta'=-\infty}^{\infty}\int_{\Theta''=-\infty}^{\infty}\rho(r,\Theta,r'=0,\Theta',r'',\Theta'')d\Theta''\,d\Theta'\,d\Theta \\ &= \frac{r^{3/2}\left[\left(3b_2^2-b_0b_4\right)r+2b_0b_2r''\right]^{1/2}}{8\sqrt{\pi}\,b_0b_2^{3/2}\left(b_0b_4-b_2^2\right)^{1/2}}\exp\left\{\frac{\left[\left(3b_2^2-b_0b_4\right)r+2b_0b_2r''\right]^2}{16b_0b_2^2\left(b_0b_4-b_2^2\right)} - \frac{b_4r^2+2b_2rr''+b_0(r'')^2}{2\left(b_0b_4-b_2^2\right)}\right\} \\ &\quad\cdot\left[I_{-1/4}\left(\frac{\left[\left(3b_2^2-b_0b_4\right)r+2b_0b_2r''\right]^2}{16b_0b_2^2\left(b_0b_4-b_2^2\right)}\right) + I_{1/4}\left(\frac{\left[\left(3b_2^2-b_0b_4\right)r+2b_0b_2r''\right]^2}{16b_0b_2^2\left(b_0b_4-b_2^2\right)}\right)\right]\end{aligned} \tag{25}$$

A change of variables yields the pdf of $(r,\Theta,r',\Theta',r'',\Theta'')$, found in (24) at the top of the page. The pdf $\rho(r,r'=0,r'')$ is then found in (25) at the top of the page, where $I_{\pm1/4}(\cdot)$ is the modified Bessel function of the first kind of order $\pm1/4$. After substitution of the expressions for b_0,b_2,b_4 and the change of variables $x = r''/[\sqrt{b_0}(2\pi/\lambda)^2]$, $y = r/\sqrt{b_0}$, (21) now becomes

$$\begin{aligned}\mathrm{ZCR}_{r'(x)} = \frac{2\sqrt{\pi}}{\lambda}\int_0^\infty\int_0^\infty & xy^{3/2}(3y/8+x)^{1/2} \\ &\cdot\exp\left\{2(3y/8+x)^2-3y^2/2-4xy-4x^2\right\} \\ &\cdot\left[I_{-1/4}\left(2(3y/8+x)^2\right)+I_{1/4}\left(2(3y/8+x)^2\right)\right]dx\,dy.\end{aligned} \tag{26}$$

Equation (26) implies that the ZCR does not depend on the average received power b_0. Numerical integration of (26) yields $\mathrm{ZCR}_{r'(x)} \approx 1.51/\lambda$. The mean distance between adjacent local minima of $g(x)$ is then $k\lambda = 1/\mathrm{ZCR}_{r'(x)} \approx 0.662\lambda$.

ACKNOWLEDGMENT

The authors would like to thank Prof. M. Vetterli for valuable suggestions and Dr. Z. Cvetković who reviewed the paper and provided helpful comments.

REFERENCES

[1] W. C. Jakes, *Microwave Mobile Communications.* New York: Wiley, 1974.
[2] M. D. Austin and G. L. Stüber, "Velocity adaptive handoff algorithms for microcellular systems," *IEEE Trans. Veh. Technol.*, vol. 43, pp. 549–561, Mar. 1994.
[3] A. Sampath and J. M. Holtzman, "Estimation of maximum Doppler frequency for handoff decisions," in *Proc. IEEE Vehicular Technology Conf.*, 1993, pp. 859–862.
[4] M. D. Austin and G. L. Stüber, "Eigen-based Doppler estimation for differentially coherent CPM," *IEEE Trans. Veh. Technol.*, vol. 43, pp. 781–785, Mar. 1994.
[5] J. Lin and J. G. Proakis, "A parametric method for Doppler spectrum estimation in mobile radio channels," in *Proc. 27th Annu. Conf. Info. Sci. Syst.*, Baltimore, MD, Mar. 25–27, 1993, pp. 875–880.
[6] J. M. Holtzman and A. Sampath, "Adaptive averaging methodology for handoffs in cellular systems," *IEEE Trans. Veh. Technol.*, vol. 44, pp. 59–66, Jan. 1995.
[7] M. Hellebrandt, R. Mathar, and M. Scheibenbogen, "Estimating position and velocity of mobiles in a cellular radio network," *IEEE Trans. Veh. Technol.*, vol. 46, pp. 65–71, Jan. 1997.
[8] D. C. Cox, "Universal digital portable radio communication," in *Proc. IEEE*, vol. 75, pp. 436–477, Apr. 1987.
[9] M. Gudmundson, "Correlation model for shadow fading in mobile radio systems," *Electron. Lett.*, vol. 27, no. 23, pp. 2145–2146, 1991.
[10] S. Mallat and W. L. Hwang, "Singularity detection and processing with wavelets," *IEEE Trans. Inform. Theory*, vol. 38, no. 2, pp. 617–643, 1992.
[11] I. Daubechies, *Ten Lectures on Wavelets.* Philadelphia, PA: SIAM, 1992.
[12] M. Vetterli and J. Kovačević, *Wavelets and Subband Coding.* Englewood Cliffs, NJ: Prentice-Hall, 1995.
[13] Z. Cvetković and M. Vetterli, "Discrete-time wavelet extrema representation: Design and consistent reconstruction," *IEEE Trans. Signal Processing*, vol. 43, no. 3, pp. 681–693, 1995.
[14] S. O. Rice, "Statistical properties of a sine wave plus random noise," *Bell Syst. Tech. J.*, vol. 27, pp. 109–157, 1948.

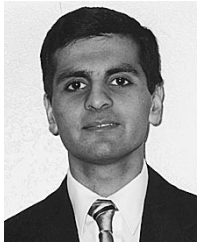

Ravi Narasimhan received the B.S. degree (with highest honors) in electrical engineering and the Certificate of Distinction from the University of California at Berkeley, in 1995, and the M.S. degree in electrical engineering from Stanford University, Stanford, CA, in 1996. He secured the first rank in the Ph.D. qualifying examination in electrical engineering at Stanford University, where he is nearing completion of the Ph.D. degree.

His research interests include wireless communication, signal processing, and wavelet analysis.

Mr. Narasimhan is a member of Phi Beta Kappa and Golden Key National Honor Society. In 1995, he received the Warren Y. Dere Memorial Prize from the University of California at Berkeley. He also received the Best Student Paper Award for the United States at the IEEE International Symposium on Personal, Indoor, and Mobile Radio Communications (PIMRC), in September 1998.

Donald C. Cox (S'58–M'61–SM'72–F'79) received the B.S. and M.S. degrees in electrical engineering from the University of Nebraska, in 1959 and 1960, respectively, and the Ph.D. degree in electrical engineering from Stanford University, Stanford, CA, in 1968. He received an Honorary Doctor of Science from the University of Nebraska in 1983.

From 1960 to 1963, he did microwave communications system design at Wright-Patterson AFB, OH. From 1963 to 1968, he was at Stanford University doing tunnel diode amplifier design and research on microwave propagation in the troposphere. From 1968 to 1973, his research at Bell Laboratories, Holmdel, NJ, in mobile radio propagation and on high-capacity mobile radio systems provided important input to early cellular mobile radio system development and is continuing to contribute to the evolution of digital cellular radio, wireless personal communications systems, and cordless telephones. From 1973 to 1983, he was Supervisor of a group at Bell Laboratories that did innovative propagation and system research for millimeter-wave satellite communications. In 1978, he pioneered radio system and propagation research for low-power wireless personal communications systems. At Bell Laboratories, in 1983, he organized and became Head of the Radio and Satellite Systems Research Department that became a Division in Bell Communications Research (Bellcore) with the breakup of the Bell System in 1984. He was Division Manager of that Radio Research Division until it again became a department in 1996. He continued as Executive Director of the Radio Research Department where he led, and contributed to research on all aspects of low-power wireless personal communications, entitled Universal Digital Portable Communications (UDPC). He was instrumental in evolving the extensive research results into specifications that became the U.S. Standard for Wireless or Personal Access Communications System (WACS or PACS). In September 1993, he became a Professor of Electrical Engineering and Director of The Center for Telecommunications at Stanford University, where he continues to pursue research on wireless mobile and personal portable communications. He was appointed Harald Trap Friis Professor of Engineering in 1994. He is the author and coauthor of many papers, conference presentations, including many invited and several keynote addresses and books. He has been granted 13 patents.

Dr. Cox is a member of Sigma Xi, Sigma Tau, Eta Kappa Nu, Phi Mu Epsilon, a member of the National Academy of Engineering, a member of Commissions B, C, and F of USNC/URSI, and was a member of the URSI Intercommission Group on Time Domain Waveform Measurements (1982–1984). He is a Registered Professional Engineer in the States of Ohio and Nebraska. He is a Fellow of AAAS and the Radio Club of America. He was an Associate Editor of the IEEE TRANSACTIONS ON ANTENNAS AND PROPAGATION (1983–1986) and a member of the Administrative Committee of the IEEE Antennas and Propagation Society (1986–88). He was the corecipient of the 1983 International Marconi Prize in Electromagnetic Wave Propagaion (Italy) and was awarded the 1993 IEEE Vehicular Technology Society Paper of the Year Award, the 1985 IEEE Morris E. Leeds Award, the 1990 IEEE Communications Magazine Prize Paper Award, the 1991 Bellcore Fellow Award, the 1992 IEEE Communications Society L. G. Abraham Prize Paper Award, and the 1993 IEEE Alexander Graham Bell Medal "for pioneering and leadership in personal portable communications."